



HAL
open science

Synthesis of magnetic multi walled carbon nanotubes hydrogel nanocomposite based on poly (acrylic acid) grafted onto salep and its application in the drug delivery of tetracycline hydrochloride

Ghasem Rezanejade Bardajee, Mahdiah Sharifi, Homeira Torkamani, Cedric Vancaeyzeele

► To cite this version:

Ghasem Rezanejade Bardajee, Mahdiah Sharifi, Homeira Torkamani, Cedric Vancaeyzeele. Synthesis of magnetic multi walled carbon nanotubes hydrogel nanocomposite based on poly (acrylic acid) grafted onto salep and its application in the drug delivery of tetracycline hydrochloride. *Colloids and Surfaces A: Physicochemical and Engineering Aspects*, 2021, 616, pp.126350. 10.1016/j.colsurfa.2021.126350 . hal-03230731

HAL Id: hal-03230731

<https://hal.science/hal-03230731>

Submitted on 10 Mar 2023

HAL is a multi-disciplinary open access archive for the deposit and dissemination of scientific research documents, whether they are published or not. The documents may come from teaching and research institutions in France or abroad, or from public or private research centers.

L'archive ouverte pluridisciplinaire **HAL**, est destinée au dépôt et à la diffusion de documents scientifiques de niveau recherche, publiés ou non, émanant des établissements d'enseignement et de recherche français ou étrangers, des laboratoires publics ou privés.



Distributed under a Creative Commons Attribution - NonCommercial 4.0 International License

1 **Synthesis of magnetic multi walled carbon nanotubes hydrogel nanocomposite based on poly (acrylic**
2 **acid) grafted onto salep and its application in the drug delivery of Tetracycline hydrochloride**

3
4 **Ghasem Rezanejade Bardajee,^{a, 1} Mahdieh Sharifi,^a Homeira Torkamani^a, Cedric Vancaeyzeele^{b, 2}**
5

6 ^a *Department of Chemistry, Payame Noor University, PO BOX 19395-3697, Tehran, Iran*

7 ^b *Laboratoire de Physicochimie des Polymeres et des Interfaces (LPPI), I-Mat, CY Cergy Paris Université, France*
8

9 **Abstract**

10 Current discovery of different modifications of multi walled carbon nanotubes has motivated research for
11 their potential applications in various field such as adsorbent materials, and drug delivery. Many different
12 modified carbon nanotubes have been achieved, including combinations with iron oxide nanoparticles
13 (NPs) for their unique properties including magnetic properties, nontoxicity, biocompatibility and
14 capability which have considerable impact on the delivery of the drug at the targeted area. However, one
15 of the disadvantages of this nanocomposite in biological fluids is that iron oxide NPs might be quickly
16 cleared by the bloodstream before realization of their targets. In order to overcome this obstacle, polymers
17 could be used as stabilizer to achieve a highly stable NPs@MWCNT composite. As a result, a magnetic
18 multi walled carbon nanotube hydrogel nanocomposite based on poly (acrylic acid) grafted onto salep was
19 synthesized and then fully characterized by using FTIR spectroscopy, thermogravimetric analysis, EDAX
20 spectrum, SEM, TEM, AFM images, and vibrating sample magnetometer (VSM) and synthesis mechanism
21 was suggested. Besides, swelling kinetics and loading and releasing of tetracycline hydrochloride as a
22 model drug in various conditions were also investigated.

23

24 **Keywords**

25 Magnetic nanocomposite, Multi walled carbon nanotubes, Hydrogel, Salep, Drug delivery
26
27
28
29
30
31
32
33
34

¹Corresponding author. Tel.: +98 21 22458309; fax: +98 21 22458315.

E-mail address: rezanejad@pnu.ac.ir

²Corresponding author. E-mail address: cedric.vancaeyzeele@cyu.fr

35

36

37 1. Introduction

38

39 Since carbon nanotubes (CNTs) were discovered in 1991, they have come under extreme multidisciplinary
40 research due to their unique physical and chemical properties. As CNTs have the features such as single-
41 wall (SWCNTs) or multiwall (MWCNTs) structures, unique size distributions, novel hollow-tube buildings
42 and high specific surface areas, they gain applications in many fields such as photocatalysis, medicine,
43 nanoscale electronics, hydrogen storage, mechanical systems and SEM probes [1-5]. To reaches these
44 applications, CNTs were decorated with various functional species. Specifically, multi-walled carbon
45 nanotubes (MWCNTs) were assembled with iron oxide NPs to meet the requirement for applications in
46 drug delivery due to their unique properties such as nontoxicity, biocompatibility and capability to deliver
47 the drug at the targeted area [6-8]. They promote magnetic properties to the composite but also sometimes
48 change other properties like mechanical, thermal and acoustic properties. In principle, magnetic
49 nanoparticles are of great interest from a wide range of aspects, including magnetic resonance imaging,
50 magnetocaloric effect, catalysis, drug release, etc. However, in biological fluids, a lack of colloidal stability
51 is a major disadvantage of iron oxide NPs that might be quickly cleared from the bloodstream before
52 realization of their targets.

53 So, we assumed that a bio-based polymeric hydrogel, involved in wide variety of biomedical applications,
54 could solve this difficulty and lead to stable nanocomposite [7]. Hydrogels first reported in the early 60's
55 [9], are hydrophilic polymers with three-dimensional and cross-linked structure [10]. Hydrogels are divided
56 into two categories based on their origin: synthetic hydrogels obtained from acrylic monomers or natural
57 superabsorbent hydrogels [11]. A lack of biocompatibility and slower degradation rates are the most
58 disadvantages of synthetic hydrogels in compare of natural hydrogels [12-15]. These last are usually
59 prepared by the bonding reaction of acrylic monolayers on a natural polymer scaffold in the presence of a
60 radical initiator and a crosslinking agent. Due to their abundance, renewability, diversity, cheapness, non-
61 toxicity, and most importantly, biodegradability and biocompatibility of their natural components, natural
62 hydrogels are more used than synthetic hydrogels. The generally used biopolymers for preparing hydrogels
63 are polysaccharides such as chitosan, alginate, carrageenan or salep [11]... Salep is extracted from tubers
64 of Orchis, Ophyris, Serapias, Platanthera, or Dactylorhiza [16]. It is a valuable source of glucomannan (16
65 to 60%), which is used as a fibrous substance in the treatment of gastrointestinal disorders and as an antidote
66 because it binds to toxins in the gastrointestinal tract and expels them before they enter the bloodstream
67 [17-20]. Due to these characteristics, salep has been commonly used as a drug delivery carrier [21, 22]. So,
68 we described in this article the development of magnetic salep based hydrogels with capacity to control the
69 drug release by external magnetic field that seems to be a great value added in comparison with traditional
70 pH or temperature sensitive smart materials [23, 24].

71 However, it is difficult to get a homogeneous distribution of magnetic nanoparticles within hydrogel
72 matrices. Up to now, different methods have been reported for synthesis of magnetic MWCNTs
73 (MMCNTs) such as layer-by-layer assembly, electrostatic attraction, hydrothermal, and direct
74 precipitating. They finally result in that explained two different methods in terms of combination of the
75 magnetic materials with the CNTs: (1) encapsulating MNPs in CNTs or (2) attaching MNPs on the surface
76 of CNTs. We preferred the direct in situ chemical precipitation method due to technically simple and
77 sufficient adsorption on MWCNTs, good magnetization of the resulting nanocomposites and therefore a
78 convenient separation process by an external magnet [24, 25].

79 Accordingly, the aim of this study is to improve of magnetic hydrogels by synthesis of a novel magnetic
80 multi walled carbon nanotubes hydrogel based on poly (acrylic acid) grafted onto salep. The main target is
81 the investigation impact of MMCNTs and salep biopolymers on the swelling, and drug release behavior.
82 Tetracycline hydrochloride (TCH) as one of the classes of antimicrobials drug and good water solubility

83 was select as a model drug. The reasonable pH- and magnetic-responsiveness introduces this magnetic
84 hydrogel as suitable candidate for potential carriers in drug delivery systems.

87 2. Experimental Section

89 2.1. Materials

91 Salep ($M_n = 1.17 \times 10^6$ g/mol, $M_w = 1.64 \times 10^6$ g/mol (high M_w), PDI = 1.39, eluent = water, flow rate =
92 1 mL/min, acquisition interval = 0.43 s from GPC results) was purchased as a powder from a supplier in
93 Kordestan, Iran. Ethanol was sourced from domestic companies. Acrylic acid (AA), ammonium persulfate
94 (APS), Iron (II) chloride tetrahydrate ($\text{FeCl}_2 \cdot 4\text{H}_2\text{O}$), Iron (III) chloride hexahydrate ($\text{FeCl}_2 \cdot 6\text{H}_2\text{O}$) and N-
95 N'-methylenebisacrylamide (MBA) were provided by Merck, Germany. Potassium hydrogen phthalate and
96 potassium phosphate were purchased from Luba Chemie. Tetracycline hydrochloride was bought from
97 Alborz Daroo Company. Multi-walled carbon nanotubes were received from US Research Nanomaterials,
98 Inc. and used without further purification. Double distillation water (DDW) was used to prepare and
99 measure the water adsorption rate of MMWCNT / Hydrogel nanocomposite.

101 2.2. Apparatus

103 FT-IR spectra of samples in the form of KBr pellets were recorded using a Jasco 4200 FT-IR. UV spectra
104 were prepared with the Shimadzu UV-visible 1650 PC. The pH meter from AZ Instrument Corp. was used
105 to investigate the behavior of the samples at different pHs. Thermal decomposition (TGA) experiments in
106 nitrogen atmosphere were performed by pyrisDiamand TG / DTA. The temperature efficiency of this device
107 was 25 to 750 °C at 10 °C/min. Scanning electron microscope (SEM), TESCAN model, has been used to
108 study the morphology of superabsorbent surfaces. The Camcan mv2300 X-ray scattering spectrum (EDX)
109 was used to determine the elemental composition of the sample. Transmission electron microscope (TEM),
110 Zeiss LEO906 model at an accelerating high voltage up to 120 kV, was used to obtain particle size. 0.01 g
111 MMWCNT / hydrogel powder was dispersed in 2 mL water. After 5 min ultrasonication, 1 mL of solution
112 put on carbon- grids and allowed to dry thoroughly before viewing by TEM. To obtain a virtual image of
113 the surface with nanometer resolution, the DM-95-50E Atomic Force Microscope (AFM) from DME was
114 used. The magnetization and hysteresis loop were measured at room temperature using a vibrating sample
115 magnetometer (VSM) (Model 880 from ADE technologies USA).

117 2.3. Preparation of Magnetic Multi Walled Carbon Nanotubes (MMWCNT)

119 The synthesis of MMWCNT was conducted by direct precipitating method. This method causes higher
120 magnetization of these nanocomposites simply because FeCl_2 used directly and the quantity of Fe_3O_4
121 deposited on MWNTs was greater [26]. For this reason, initially a solution of $\text{FeCl}_3 \cdot 6\text{H}_2\text{O}$ (3.5 g in 20 mL
122 water) and $\text{FeCl}_2 \cdot 4\text{H}_2\text{O}$ (0.2 g in 20 mL water) poured in 200 mL degassed water and set the temperature
123 at 50 °C. Then 10 mL water containing 1.0 g of multi-walled carbon nanotube was added to the solution
124 during stirring and the temperature was increased to 70 °C. In the next step, 8 mL of ammonia solution was
125 added to reaction under same reflux condition for 1 h. Finally, the obtained product was collected with a
126 magnet and wash with water 3 times and dried in oven at 70 °C for 72 h.

2.4. A typical optimum procedure for synthesis of MMWCNT/hydrogel nanocomposite via hydrothermal method

At this stage, APS is used as the initiator and AA as the monomer. MBA has been used as a crosslinking agent and salep has been used as a substrate for the synthesis of MMWCNT / hydrogel nanocomposites. Typically, 1.0 g salep was dissolved in 70 mL hot DDW (70 °C). Then reactor was settled in a hot water bath at 70 °C and mix with a mechanical stirrer at 600 rpm for 10 minutes. After this time, 0.05 g of prepared MMWCNT and 5 mL of the tetracycline hydrochloride (0.1 M) drug were mixed to each other for 30 min, added to homogenous salep solution, and mixed for 20 minutes with a mechanical stirrer. Then 2 mL AA and 0.06 g MBA mixed with this solution. Finally, after homogenizing, 0.03 g of APS were added to the reaction allowed to complete for 30 min. Then, the reaction mixture was cooled to room temperature and the product was dewatered by ethanol (50 mL) and then the dewatered nanocomposite filtered and dried in oven at 50 °C for 24 h. Finally, in grinding step, the obtained powder passed through a mesh sieve No. 60 and it stored for other experiments.

2.5. Swelling Measurement

A gravimetric method was used to determine the swelling of nanocomposite in water. For this case, a tea bag (i.e. a 100 mesh nylon screen) containing an accurately dry powdered sample (0.2 ± 0.001 g) with average particle sizes between 40-60 mesh was immersed entirely in distilled water (200 mL) and allowed to soak for 3 h at the room temperature. The equilibrium swelling (ES) capacity was measured twice at the room temperature using the following formula (Eq. 1):

$$ES \text{ (g/g)} = (W_2 - W_1)/W_1 \quad (1)$$

where W_1 and W_2 are the weights of dry and swollen gels, respectively.

The water adsorption rate of MMWCNT / hydrogel nanocomposite over time was studied by adding 0.02 g of hydrogel into a tea bag that placed in 200 mL of distilled water. Then the water absorption was measured at specified times. A similar process was investigated under magnetic field and hydrogel without MMWCNT.

To investigate the effect of temperature on the amount of hydrogel water absorption, 0.02 g of hydrogel was added into a tea bag and placed in a beaker containing 200 mL of water in a bath with the desired temperature and water absorption was evaluated after three hours.

pH dependence of the swelling was measured by interaction of certain amounts of the hydrogel samples (0.02 g) in solutions (200 mL) at different pH. The various solutions were fixed to the desired pH value by addition of diluted HCl or NaOH. The On-Off switching by pH was carried out at buffered solutions with pH=2 and pH=9 with 0.01 molar concentrations.

2.6. Drug release

For drug releasing study, the MMWCNT / hydrogel nanocomposite (0.2 ± 0.01 g) was dispersed in 50.0 of buffer solutions at different pHs in a rotary shaker (200 rpm). At regular intervals, 2.0 mL of the solution was removed from the sample and the UV spectrum was taken and replaced with 2.0 mL of fresh solution. Finally, the amount of drug releasing was measured at 485 nm by UV-vis spectrophotometer using a calibration curve of the drug at different concentrations.

3. Results and Discussions

3.1. Synthesis mechanism and spectral characterization

At the first step, ammonium persulfate (APS), as an initiator, is decomposed under heating to produce sulfate anion-radical. Then, the anion-radical abstracts hydrogen from one of the functional groups inside chains (i.e. CH, OH) of the salep substrate to form corresponding radical [26]. The oxidation and reduction system of persulfate-saccharide causes a radical polymerization reaction in which the acrylic acid monomer (AA) is converted to polyacrylic acid (PAA) and at the same time grafts to the polysaccharide chain. In addition, crosslinking reaction was carried out in the presence of a crosslinker, MBA, so that the MMWCNT / hydrogel nanocomposite was obtained (see Fig. 1).

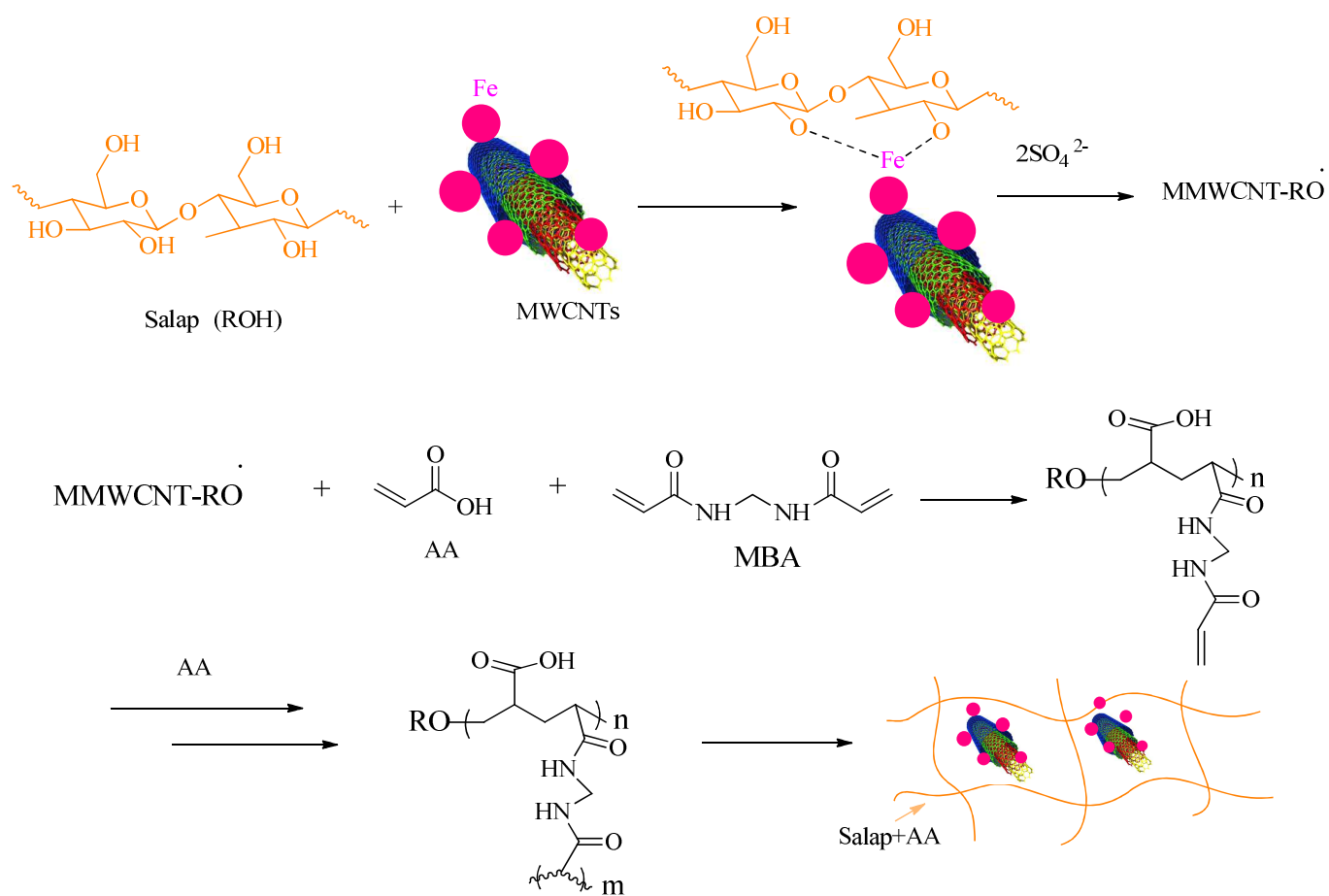
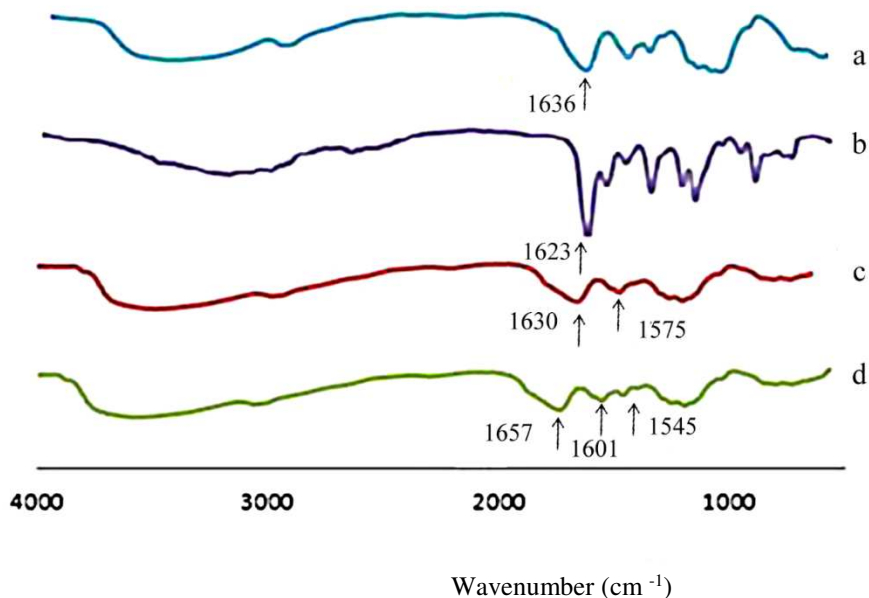


Fig. 1. Proposed mechanism pathway for the synthesis of MMWCNT / hydrogel nanocomposite

Infrared spectroscopy was used to confirm the chemical structure of the grafted products. Fig. 2 shows the FT-IR spectra of non-magnetic carbon nanotube hydrogel, MMWCNT / hydrogel nanocomposite, AA and salep. Fig. 2a shows the spectrum related to salep (mainly glucomannan). The peak in the region of 1633 cm^{-1} can be attributed to the stretching vibrations of the carbonyl group ($C=O$) in glucomannan of salep. In Fig. 2b, which is related to AA, the peak in the 1623 cm^{-1} region is related to the stretching vibrations of carboxyl groups. Fig. 2c, which deals with hydrogels without magnetic carbon nanotubes, shows two absorption peaks in the region of 1575 cm^{-1} and 1630 cm^{-1} . These peaks are related to the stretching vibrations of the carbonyl groups of the salep biopolymer chains and PAA, both of which are present simultaneously in the hydrogel. In Fig. 2d, which is related to the MMWCNT / hydrogel nanocomposite, the indicator peaks of the stretching vibrations of the carbonyl groups mentioned above are present,

202 although these peaks have a slight displacement towards a higher wave number. The major peak in the
203 region of 1545 cm^{-1} is related to the stretching vibrations of double bonds of carbon nanotubes. In addition,
204 in all spectra, the broad bands at $3300\text{-}3000\text{ cm}^{-1}$ is related to the stretching vibrations of the hydroxyl
205 group.
206
207
208



209 Fig. 2. FT-IR spectra of (a) salep, (b) AA, (c) hydrogel, and (d) MMWCNT / hydrogel nanocomposite.
210
211

212 TGA curves of hydrogel without MMWCNTs and with MMWCNTs at the temperature range of 25 to 750
213 °C are shown in Fig. 3. In the case of hydrogel without MMWCNTs, 11% weight loss between 25 °C and
214 225 °C is due to loss of H₂O. Moreover, 40% weight loss between 225 and 325 °C is due to the degradation
215 of the hydrogel structure and releases of CO₂ and H₂O, especially resulting from the decomposition of
216 salep. The third step contains 30% weight loss between 425 and 475 °C, is assigned to the degradation of
217 poly (acrylic acid) in hydrogel. On the other hand, hydrogel with MMWCNTs showed a lower weight loss
218 than hydrogel without MMWCNTs in same temperature range. Indeed, the difference in the residual weight
219 of 20 wt% corresponds to the combination of thermally stable iron oxide nanoparticles and MWCNTs of
220 the MMWCNTs composite [27].
221

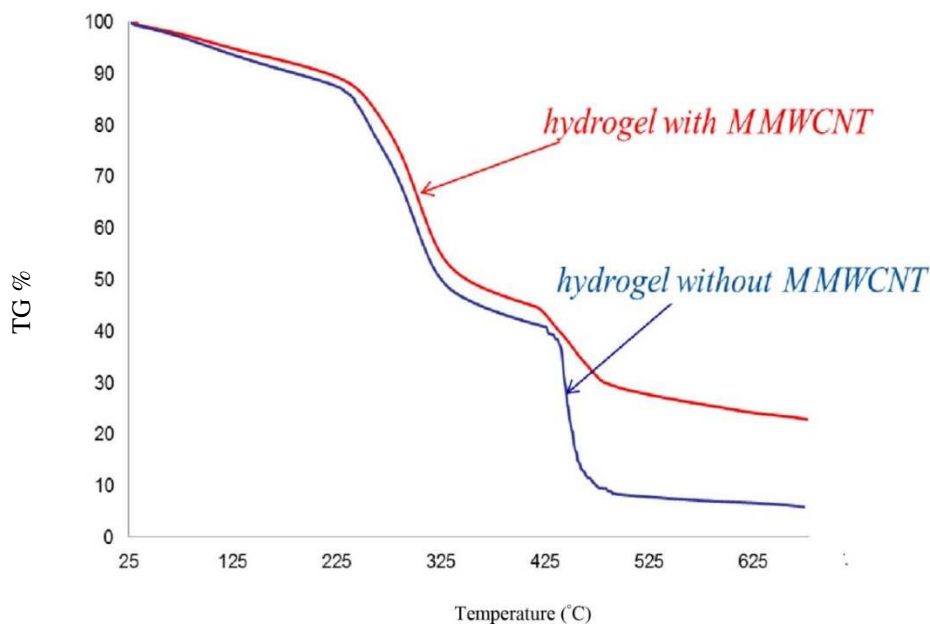


Fig. 3. TGA curves of hydrogel without MMWCNTs and with MMWCNTs

Table 1. Thermo-gravimetric analysis (TGA) of hydrogel without MMWCNTs and with MMWCNTs

region	Hydrogel without MMWCNT		Hydrogel with MMWCNT	
	Range °C	Weight loss (%)	Range °C	Weight loss (%)
1 st	25-225	11	25-225	8
2 nd	225-325	40	225-325	38
3 rd	425-475	30	425-475	15

Scanning electron microscopy (SEM) images have been used to study the morphology of MMWCNT / hydrogel nanocomposite surfaces. As Fig. 4a and 4b shows, the synthesized nanocomposite hydrogel has layered surfaces and holes in its structure and has a relatively porous structure. The porosity of the hydrogel networks is one of the factors promoting the absorption capability of the hydrogel, so the rate of swelling of the hydrogel can be attributed to its structure [28, 29]. EDX analyses were carried out to corroborate elements used in the hydrogel composition. An EDX spectrum of MMWCNT / hydrogel is described in Fig. 4c. The spectrum indicates characteristic peaks of Fe, O, and C elements in the MMWCNT / hydrogel with Fe typical of the iron oxide particles anchored on MWCNT.

For TEM observation, the nanocomposite hydrogel (0.1 g in 2 mL water) was sonicated for 5 minutes to disrupt the polymer matrix and disperse the magnetic nanotube in water solution. A drop of this solution was casted in a TEM copper grid to evaluate the distribution of carbon nanotubes in the polymer matrix and the results have been shown in Fig. 4d and 4e with their size distribution histograms. The average diameter of nanotubes in the polymer network was 6 to 8 nm. High magnification TEM image of sample (Fig. 4d) reveals the dispersion of carbon nanotubes in the hydrogel frame. Besides, the dark spot refers to iron nanoparticle. The relationship between the magnetic field and the magnetization of the MMWCNT / hydrogel at room temperature showed in Fig. 4f. The hysteresis loop of the samples confirms that the magnetic behavior of the MMWCNT / hydrogel is highly influenced by the mediating iron nanoparticles.

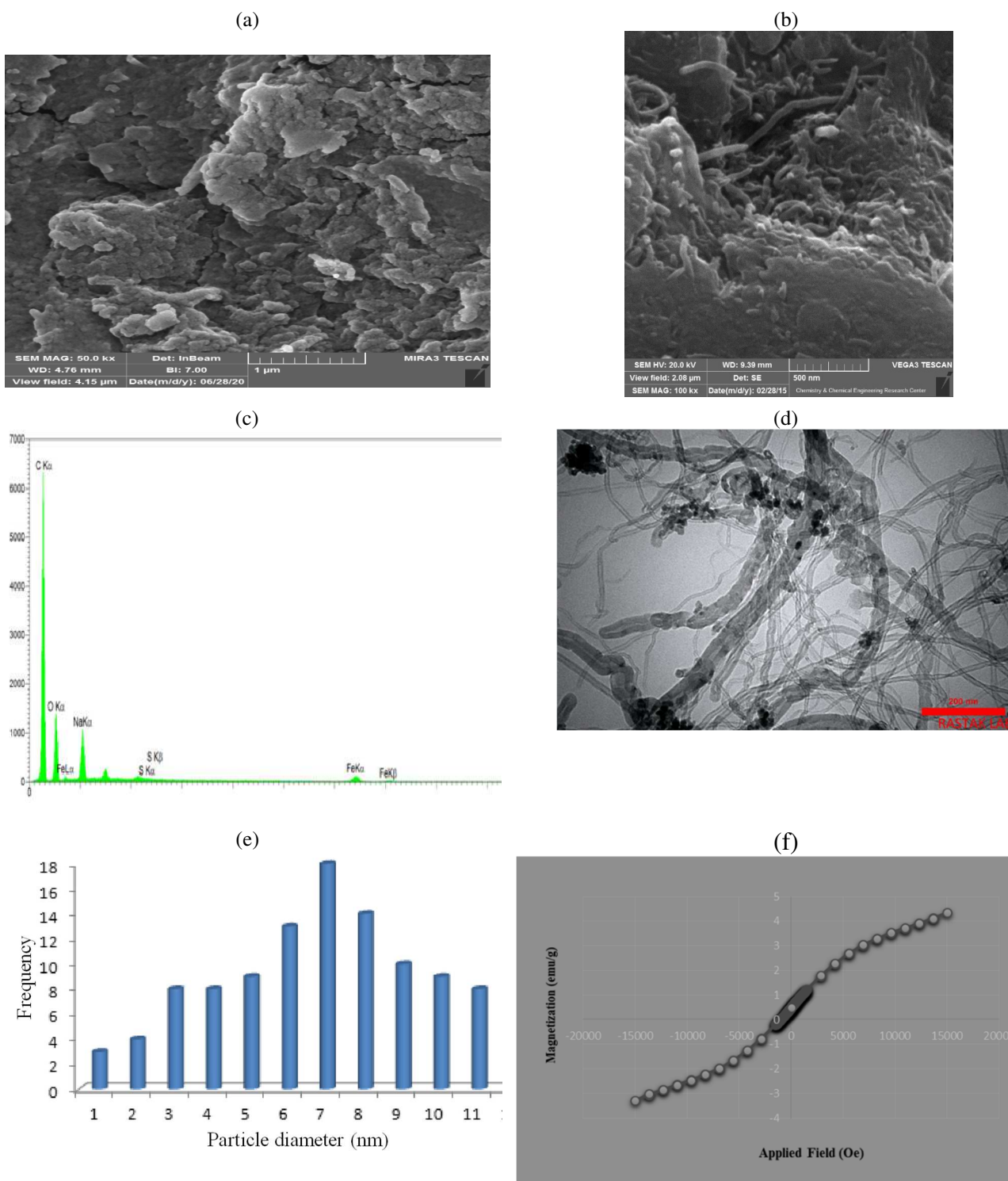


Fig. 4. a) and b) SEM image, c) EDX spectrum of the hydrogel with MMWCNTs, d) TEM image of disrupted hydrogel with MMWCNTs after sonication for 5 min, e) histogram of the MMWCNTs diameter distribution measured from the TEM image and f) Magnetic hysteresis loop for MMWCNT / hydrogel

3.2. Optimization of the grafting conditions

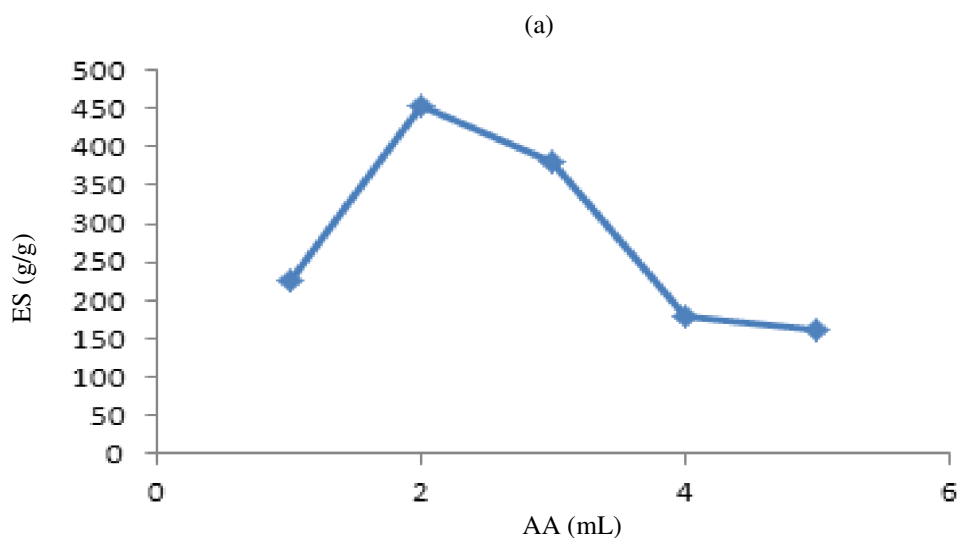
There is a strong relationship between the swelling ratio and network structure parameters. Also, different parameters can affect the final swelling capacity in hydrogels [30]. Here, the amount of monomer, crosslinking agent and initiator were systematically optimized. Besides, the environmental parameters such

260 as reaction time (swelling kinetic), temperature, dual solvents, salinity and pH sensitivity were optimized
261 to achieve MMWCNT / hydrogel nanocomposite with maximum water absorbency.

262 3.2.1. Effect of monomer, crosslinking agent and initiator

264 Fig. 5a illustrated the effect of AA amount on water uptake of the synthesized MMWCNT/hydrogel.
265 Different amounts of AA (1.485×10^{-2} – 7.27×10^{-2} mol (1–5 mL)) were used, where the maximum of
266 swelling capacity is attained at 2 mL of AA amount.

267 As the monomer concentration increases to 2 mL, water absorption increases. Due to the increase in the
268 polymerization reaction rate, the number of AA hydrophilic functional groups increases along the hydrogel
269 chains and it causes an increase in water swelling. Finally, water swelling decreases with further increase
270 in monomer concentration. Since, some of undesirable intermolecular cross-linking formed [31]. The effect
271 of MBA concentration as a crosslinking agent on water absorption of the MMWCNT/hydrogel was
272 examined by varying the MBA amount from 0.02 to 0.08 g (1.297×10^{-4} – 5.189×10^{-4} mol), whereas the
273 amount of AA was kept in optimum value (2 mL of AA) from previous experiment. As seen in Fig. 5b,
274 MBA concentration was an effective variable on the swelling behavior especially in 0.06 g region.
275 According to Flory's theory, adding the extra amount of cross-linker have effect on the generation of
276 immoderate cross-link points. As a result, the network voids for holding water are reduced and the water
277 absorption decreases [30]. Thus, the water absorption capacity was significantly decreased with increasing
278 MBA after 0.06 g. simply because, excess amount of MBA increases the extent of crosslinking of the
279 polymeric chains and decreases the free spaces between them. So, a rigid structure is formed that do not
280 have capacity to hold a large quantity of water [32]. Fig. 5c shows the effect of the initiator content (APS)
281 on the water absorbency. The water absorbency increases with increase in the initiator content from 0.025
282 to 0.09 g and then it decreases with further excess amount of APS. The relation between water absorbency
283 and concentration of APS can be related to the increase in the number of active centers (carboxylic acid)
284 on the salep backbone, which in turn results in more extensive graft copolymerization. This increase in
285 active centers makes the nanocomposite hydrogel more hydrophilic and increases the water absorption
286 capacity. The decrease in adsorption after the maximum value of APS can be attributed to some extent to
287 self-crosslinking. Another important reason can be attributed to the free radical degradation of salep that
288 can also take place at high APS levels [22]. Therefore, the optimal monomer, crosslinking agent and
289 initiator concentration were found to be 2 mL, 0.06 g, and 0.09 g respectively which was kept in further
290 analysis.



(b)

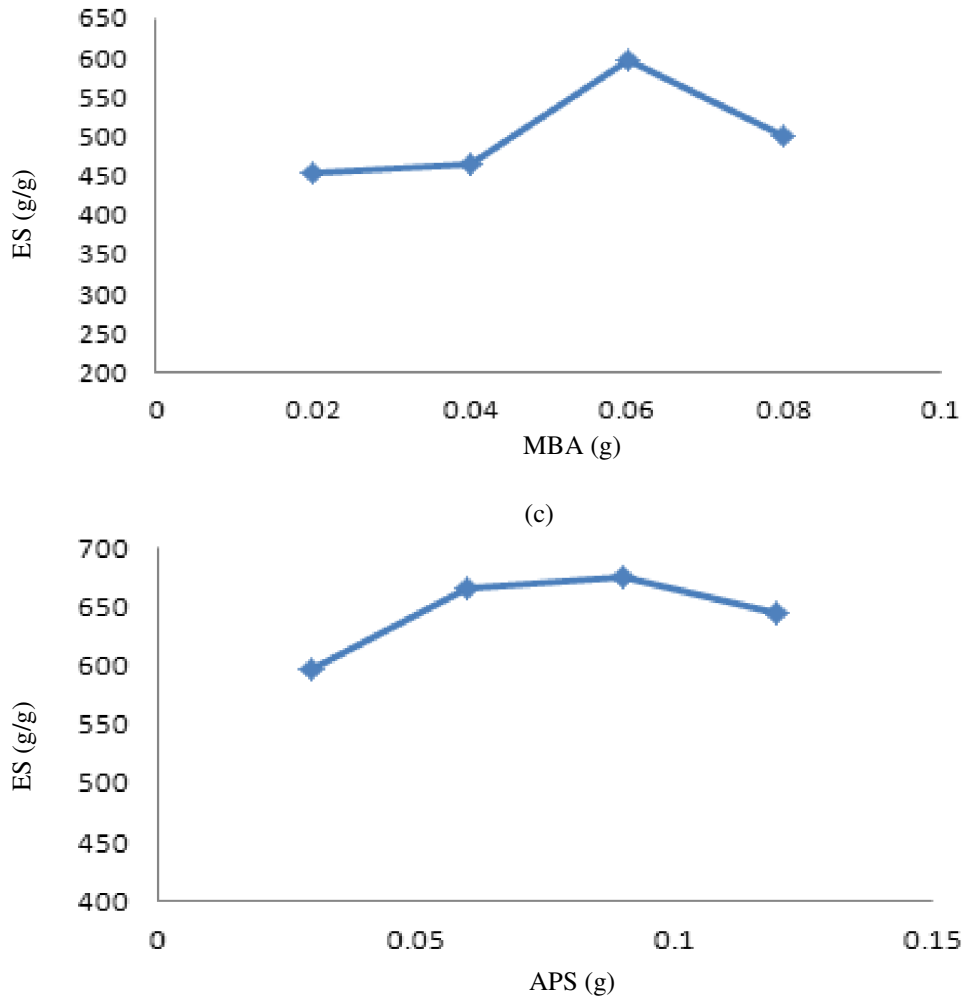


Fig. 5. Effect of a) monomer amount (reaction conditions: salep weight = 1.0 g, MBA = 1.2×10^{-4} mol, and APS= 1.3×10^{-4} mol), b) crosslinker amount (reaction conditions: salep weight = 1.0 g, AA = 2.9×10^{-2} mol, and APS = 1.31×10^{-4} mol), and c) initiator amount (reaction conditions: salep weight = 1.0 g, AA = 2.9×10^{-2} mol, and MBA= 3.8×10^{-4} mol) on equilibrium swelling capacity of the MMWCNT / hydrogel nanocomposite.

3.2.2. Effect of time (swelling kinetic)

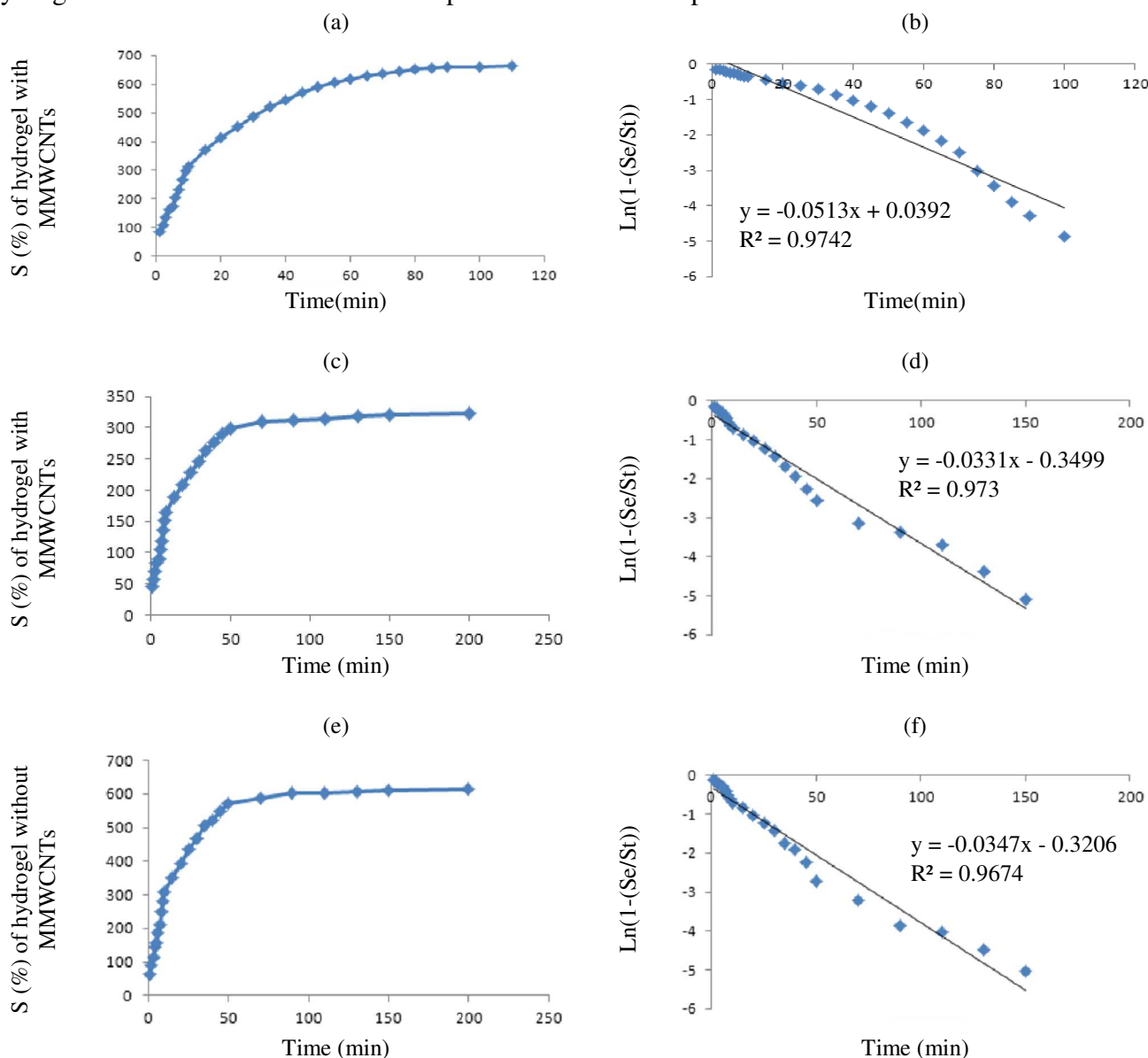
Different parameters such as swelling capacity, size distribution of powder particles, specific surface and composition of polymer affected on swelling kinetics of the hydrogels (super absorbents) [33]. Fig. 6a represents the swelling (S) behavior of MMWCNT / hydrogel in distilled water at consecutive time intervals. The water absorbency intensely increased versus time up to 60 min and then, it begins to level off. The data may be well matched with a Voigt-based Eq. (Eq. 2) [34]:

$$S_t = S_e (1 - e^{-t/\tau}) \quad (2)$$

where S_t (g/g) is swelling at time t , S_e is equilibrium swelling; t is time (min) for swelling S_t , and τ (min) stand for the rate parameter. One can obtain the rate parameter from a plot of $\ln(1 - (S_t / S_e))$ vs. time (t) using the above formula with a little rearrangement. The slope of the fitted straight line (slope = $-1/\tau$) gives the rate parameter. As one can see in Fig. 6b and using Eq. (2), the rate parameter τ for swelling of the MMWCNT / hydrogel in water is found to be 23.42 min. Fig.6c, d shows the rate parameters for swelling of the MMWCNT / hydrogel in presence of magnetic field that τ increases to 30.21 min.

316 In the presence of an external magnetic field, the MMWCNT / Hydrogel nanocomposite is trapped inside
 317 the magnetic field. Indeed, the magnet reduces the distance between the ions and produces a close packing
 318 of ions, which prevents transudation of water into MMWCNT / Hydrogel. So, swelling capacity of the
 319 hydrogel is reduced.

320 Besides, the rate parameters for swelling of the hydrogel without MMWCNT is reported around 28.21 min
 321 that showed that swelling capacity of the hydrogel without MMWCNT is reduced in compare of
 322 MMWCNT / Hydrogel (see Fig. 6e, f). Due to, more space is created by carbon nanotubes in MMWCNT /
 323 Hydrogel that increased both water absorption and water absorption rate.

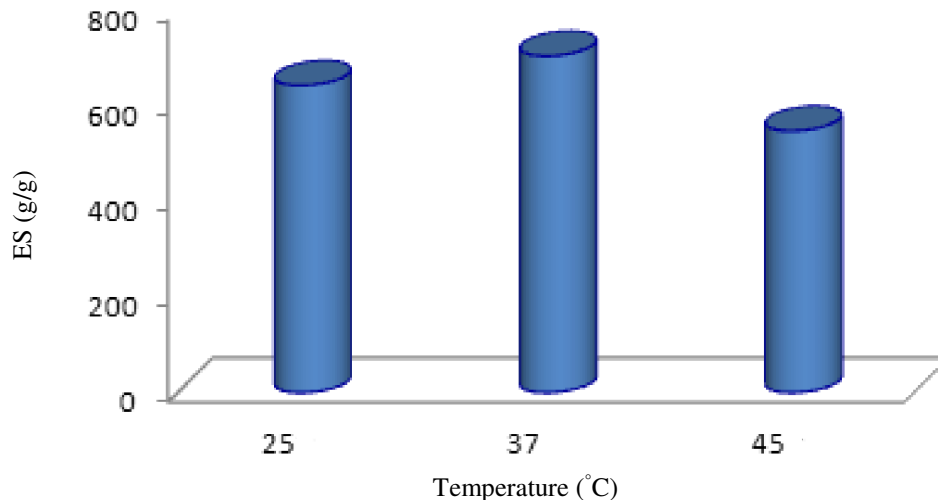


324 Fig. 6. a) The swelling kinetics and b) Voigt equation for swelling of hydrogel with MMWCNTs in distilled water. c) The
 325 swelling kinetics and d) Voigt equation for swelling of hydrogel with MMWCNTs in distilled water in present of external
 326 magnetic field e) The swelling kinetics and f) Voigt equation for swelling of hydrogel without MMWCNTs in distilled
 327 water.
 328

329 3.2.3. Effect of swelling medium temperature

330
 331 The equilibrium swelling (ES) capacity of the nanocomposite sample at different temperatures (25, 37 and
 332 45 °C) is shown in Fig. 7. The synthesized MMWCNT/hydrogel has the highest swelling at human body
 333 temperature (37 °C). At this temperature, the higher flexibility of the network chains causes better diffusion
 334 of water molecules in nanocomposite networks and consequently the water swelling increases. However,
 335

336 at higher temperatures, breaking of hydrogen bonds between functional groups (mainly hydroxyl and
337 carboxylic moieties) of hydrogel nanocomposite and water promotes a decrease in swelling capacity [35].



338
339 Fig. 7. Temperature effect of MMWCNT/hydrogel on water absorption
340

341 3.2.4. pH sensitivity and pulsatile behavior 342

343 To study the sensitivity of the MMWCNT/hydrogel to pH, the swelling capacity of the nanocomposite was
344 studied at various pHs ranging from 2.0 to 11.0. As one can see in Fig. 8a, the swelling capacity increases
345 with the increase of pH until pH = 9 and then decreases with further raising pH to 11. At pH = 9, the
346 functional groups of carboxyl groups (COOH) are converted to carboxylates anion (COO⁻). As a result, the
347 highest water adsorption of nanocomposite is observed due to the increase in electrostatic repulsion.
348 However, at pH=11, increased ionic strength of the outer solution can reduce electrostatic repulsion and
349 thereby reduced water adsorption of nanocomposite.

350 The labeled nanocomposite further exhibited reproducible swelling–deswelling cycles as demonstrated in
351 Fig. 8b. At pH = 9, the hydrogel swelled up to 809.37 g/g (%) due to anion–anion repulsive electrostatic
352 forces, while at pH = 2, it reduced within a few minutes due to the hydrogen bond-type attractive forces
353 between polymer chains.

354 This sudden and sharp swelling–deswelling behavior at different pH values makes the system highly pH-
355 responsive and efficient for tailoring pulsatile (on–off swelling) drug delivery systems. It is well known
356 that smart materials are the ones that have one or more properties that could be significantly altered in a
357 controlled fashion by external stimuli such as mechanical stress, temperature, moisture, pH, and electric or
358 magnetic fields. In brief, the hydrogel nanocomposite in question can now be considered as a truly smart
359 material.
360

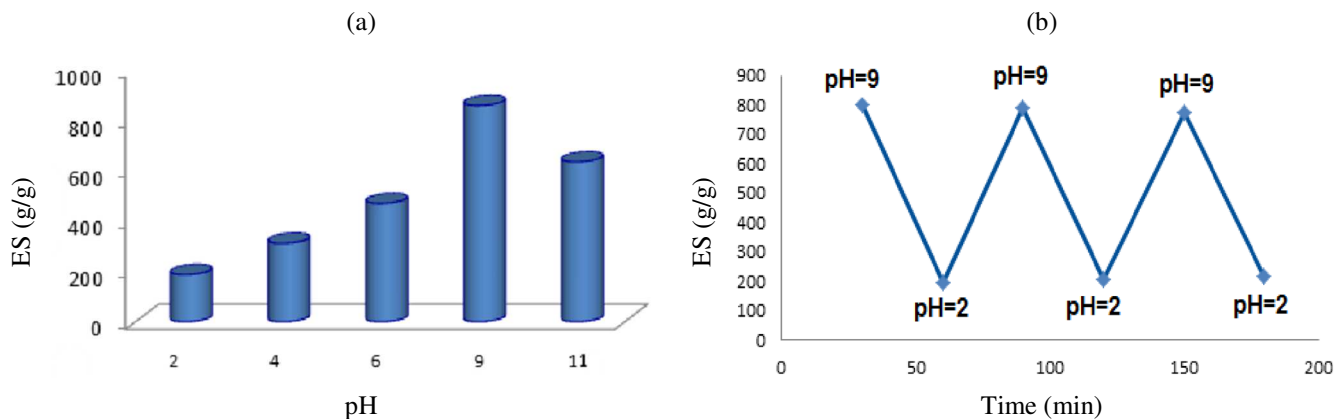
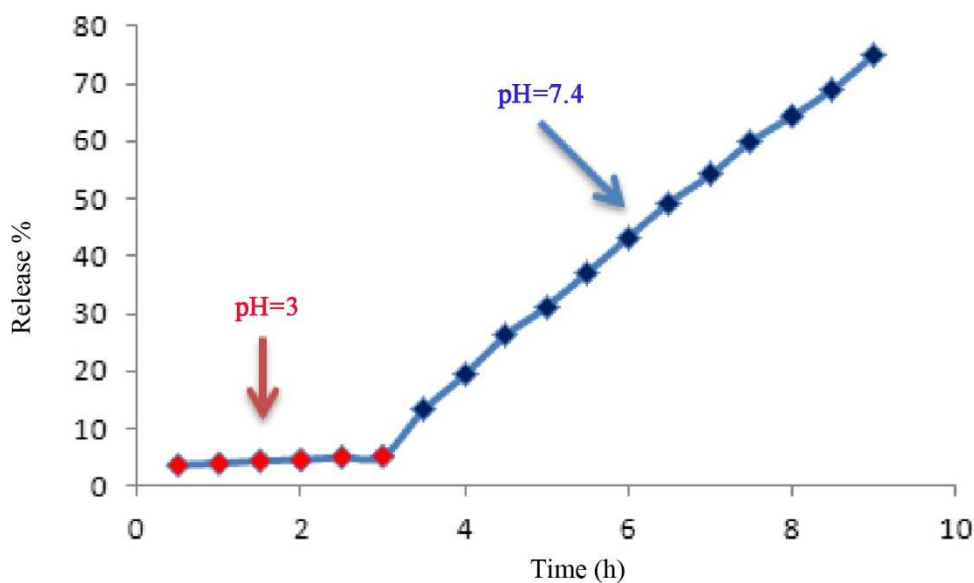


Fig. 8 a) Swelling dependency of the optimized MMWCNT/hydrogel on pH and b) on-off switching behavior of the optimized nanocomposite in pH = 9 and pH = 2.

3.3. Drug release studies

To evaluate the drug release from the nanocomposite in vitro, the tetracycline hydrochloride (TCH) loaded nanocomposite was immersed in phosphate buffers with different pHs at 37 °C and recorded the release of tetracycline by UV at regular intervals. Overall, the drug delivery tests were carried out mimicking the colon and stomach condition. At an acidic pH (similar to stomach condition), the drug release only reached 5% after 5 h with a slower release. However, to an ideal microbial effect of tetracycline the pH = 7.4 MMWCNT/hydrogel was capable of drug-controlled delivery with good properties of delayed release (see Fig. 9a). This shows that the amount of tetracycline hydrochloride release is pH dependent. Three possible interactions assumed between TCH and MMWCNTs/hydrogel which are known as followed: (a) π - π stacking interaction; (b) hydrophobic interaction; and (c) hydrogen-bonding interaction between the TCH-OH and the -COOH groups. The results showed that the release capacity was enhanced with the increment of pH. The effect of magnetic field on drug release synthesized MMWCNT/hydrogel also investigated at pH=7.4 and 37 °C (Fig. 9b). As can be seen, the amount of released drug from all samples was decreased by a factor of two by applying external MF.



(a)

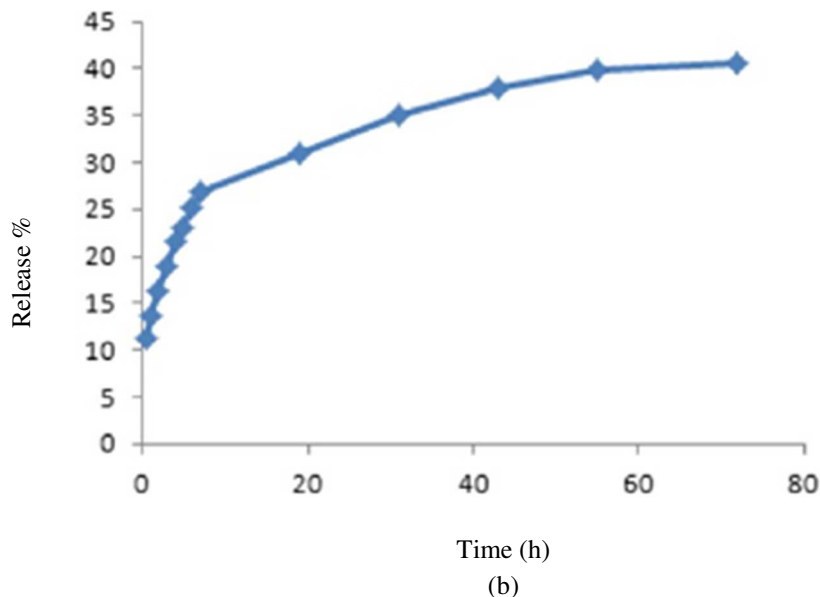


Fig 9. Release studies of tetracycline hydrochloride from MMWCNT/hydrogel at 37°C and (a) at pH 3 or 7.4 without external magnetic field (MF) and (b) at pH 7.4 with MF.

4. Conclusion

In the current work, the synthesis and swelling capacity of a new magnetic multi walled carbon nanotubes hydrogel nanocomposite based on poly (acrylic acid) grafted onto salep were described. Factors affecting the water swelling during the hydrogel synthesis (monomer concentration, MBA concentration, APS concentration) were systematically optimized and the impact of various environmental conditions (time, temperature, pHs) were examined. The nanocomposite was fully characterized and confirmed by FTIR, SEM, TEM, EDAX, TGA, and VSM. The rate parameters for swelling of the hydrogel without MMWCNT is reported around 28.21 min that showed that swelling capacity of the hydrogel without MMWCNT is reduced in compare of MMWCNT / Hydrogel. Also, the nanocomposite exhibited high sensitivity to pH. So that, the repeatable swelling–deswelling behavior of nanocomposite in pHs 2 and 9 could classify it as a smart material with potential application in pharmaceuticals. The response of the prepared nanocomposite against tetracycline hydrochloride release at different pHs made this MMWCNT / Hydrogel suitable for the drug release at pH= 7.4. The results of VSM exhibited that the MMWCNT/ hydrogel has a superparamagnetic property and it decreases release of the drug in presence of external MF.

Acknowledgments

The authors are grateful to PNU and INSF for financial support (Contract Number 46384) of this work.

References

- [1] Y. Hu, R. Jiang, J. Zhang, C. Zhang, G. Cui, Technology, Synthesis and properties of magnetic multi-walled carbon nanotubes loaded with Fe₄N nanoparticles, *Journal of Materials Science*, 34 (2018) 886-890.
- [2] H. Yan, X. Xue, Y. Fu, X. Wu, J. Dong, Three-dimensional carbon nanotubes-encapsulated Li₂FeSiO₄ microspheres as advanced positive materials for lithium energy storage, *Ceramics International*, 46 (2020) 9729-9733.

420 [3] Y. Lee, J. Yoon, H.-J. Kim, G.-H. Park, J.W. Jeon, D.H. Kim, D.M. Kim, M.-H. Kang, S.-J. Choi,
 421 Wafer-Scale Carbon Nanotube Network Transistors, *Nanotechnology*, (2020).

422 [4] X. Guo, Y. Huang, W. Yu, X. Yu, X. Han, H. Zhai, Multi-walled carbon nanotubes modified with iron
 423 oxide and manganese dioxide (MWCNTs-Fe₃O₄-MnO₂) as a novel adsorbent for the determination of BPA,
 424 *Microchemical Journal*, (2020) 104867.

425 [5] S.K. Prajapati, A. Malaiya, P. Kesharwani, D. Soni, A. Jain, Biomedical applications and toxicities of
 426 carbon nanotubes, *Drug Chemical Toxicology*, (2020) 1-16.

427 [6] P. Ghoderao, S. Sahare, P. Alegaonkar, A.A. Kulkarni, T. Bhawe, Multiwalled Carbon Nanotubes
 428 Decorated with Fe₃O₄ Nanoparticles for Efficacious Doxycycline Delivery, *ACS Applied Nano Materials*,
 429 2 (2018) 607-616.

430 [7] M.S. Amini-Fazl, R. Mohammadi, K. Kheiri, 5Fluorouracil loaded chitosan/polyacrylic acid/Fe₃O₄
 431 magnetic nanocomposite hydrogel as a potential anticancer drug delivery system, *International journal of*
 432 *biological macromolecules*, 132 (2019) 506-513.

433 [8] L.B. Sukhodub, L.F. Sukhodub, Y.I. Prylutsky, N.Y. Strutynska, L. Vovchenko, V. Soroca, N.
 434 Slobodyanik, N. Tsierkezos, U. Ritter, Composite material based on hydroxyapatite and multi-walled
 435 carbon nanotubes filled by iron: Preparation, properties and drug release ability, *Materials Science*
 436 *Engineering: C*, 93 (2018) 606-614.

437 [9] P. Gupta, K. Vermani, S. Garg, Hydrogels: from controlled release to pH-responsive drug delivery,
 438 *Drug discovery today*, 7 (2002) 569-579.

439 [10] A.S. Hoffman, Hydrogels for biomedical applications, *Advanced drug delivery reviews*, 64 (2012) 18-
 440 23.

441 [11] M.M. Khansari, L.V. Sorokina, P. Mukherjee, F. Mukhtar, M.R. Shirdar, M. Shahidi, T. Shokuhfar,
 442 Classification of hydrogels based on their source: a review and application in stem cell regulation, *JOM*,
 443 69 (2017) 1340-1347.

444 [12] M.M. ZHOURIAN, K. Kabiri, Superabsorbent polymer materials: a review, *Iranian Polymer Journal*,
 445 17 (6) (2008) 451-477.

446 [13] S. Afroz, F. Afrose, A. Alam, R.A. Khan, M.A. Alam, H. Materials, Synthesis and characterization of
 447 polyethylene oxide (PEO)—N, N-dimethylacrylamide (DMA) hydrogel by gamma radiation, *Advanced*
 448 *Composites*, 2 (2019) 133-141.

449 [14] P. Jiang, G. Li, L. Lv, H. Ji, Z. Li, S. Chen, S. Chu, Effect of DMAEMA content and polymerization
 450 mode on morphologies and properties of pH and temperature double-sensitive cellulose-based hydrogels,
 451 *Journal of Macromolecular Science, Part A*, 57 (2020) 207-216.

452 [15] F. Afrose, S. Afroz, T.S.B. Monir, M.S. Rahaman, A. Alam, R.A. Khan, M.A. Alam, Synthesis and
 453 Characterization of Hydrogel based on Poly (vinylpyrrolidone) and N-hydroxyethyl acrylamide with Agar
 454 by Gamma Radiation, *Journal of Noakhali Science and Technology University (JNSTU)*, 3 (2019) 1-7

455 [16] C. Ece Tamer, B. Karaman, O. Utku Copur, A traditional Turkish beverage: salep, *Food Reviews*
 456 *International*, 22 (2006) 43-50.

457 [17] G.R. Bardajee, A. Pourjavadi, R. Soleyman, N. Sheikh, Gamma irradiation mediated synthesis of a
 458 new superabsorbent hydrogel network based on poly (acrylic acid) grafted onto salep, *Journal of the Iranian*
 459 *Chemical Society*, 7 (2010) 652-662.

460 [18] J.K. Keithley, B. Swanson, Glucomannan and obesity: a critical review, *Alternative therapies in health*
 461 *medicine*, 11 (2005) 30-35.

462 [19] H. Chen, Q. Nie, J. Hu, X. Huang, K. Zhang, S. Pan, S. Nie, Hypoglycemic and hypolipidemic effects
 463 of glucomannan extracted from konjac on type 2 diabetic rats, *Journal of agricultural food chemistry*, 67
 464 (2019) 5278-5288.

465 [20] Z. LV, Y. WU, M. HE, Q. YAN, M. CHEN, L. FENG, J. ZHAO, B. WANG, Effect of Modified
 466 Konjac Glucomannan on Lipid Metabolism and Related Gene Expression of Schizothorax prenanti, *Journal*
 467 *of Food Science Biotechnology journal*, (2018) 18.

468 [21] G.R. Bardajee, Z. Hooshyar, One-pot synthesis of biocompatible superparamagnetic iron oxide
 469 nanoparticles/hydrogel based on salep: characterization and drug delivery, *Carbohydrate polymers*
 470 101 (2014) 741-751.

- 471 [22] G.R. Bardajee, F. Mizani, S.S. Hosseini, pH sensitive release of doxorubicin anticancer drug from gold
472 nanocomposite hydrogel based on poly (acrylic acid) grafted onto salep biopolymer, *Journal of Polymer*
473 *Research*, 24 (2017) 48.
- 474 [23] J. Zhang, Q. Huang, J. Du, Recent advances in magnetic hydrogels, *Polymer International*, 65 (2016)
475 1365-1372.
- 476 [24] D. Xiao, P. Dramou, H. He, L.A. Pham-Huy, H. Li, Y. Yao, C. Pham-Huy, Magnetic carbon nanotubes:
477 synthesis by a simple solvothermal process and application in magnetic targeted drug delivery system,
478 *Journal of Nanoparticle Research*, 14 (2012) 984.
- 479 [25] X. Song, F. Yang, X. Wang, K. Zhang, Preparation of magnetic multi-walled carbon nanotubes and
480 their application in active dye removal, *Micro Nano Letters*, 6 (2011) 827-829.
- 481 [26] G.R. Bardajee, S.S. Hosseini, C. Vancaeyzeele, Graphene oxide nanocomposite hydrogel based on
482 poly (acrylic acid) grafted onto salep: an adsorbent for the removal of noxious dyes from water, *New*
483 *Journal of Chemistry*, 43 (2019) 3572-3582.
- 484 [27] G.R. Bardajee, M. Zamani, M. Sharifi, H. Mahmoodian, Preparation of Novel Fluorescence
485 Nanosensor κ C-CdTe/ZnS Quantum Dots for High Accurate Detection of Epirubicin, *Materials Today*
486 *Communications*, (2020) 101874.
- 487 [28] X. Kang, Z. Xia, R. Chen, P. Liu, W. Yang, Effects of inorganic cations and organic polymers on the
488 physicochemical properties and microfabrics of kaolinite suspensions, *Applied Clay Science*, 176 (2019)
489 38-48.
- 490 [29] K. Kabiri, H. Omidian, S. Hashemi, M. Zohuriaan-Mehr, Synthesis of fast-swelling superabsorbent
491 hydrogels: effect of crosslinker type and concentration on porosity and absorption rate, *European Polymer*
492 *Journal*, 39 (2003) 1341-1348.
- 493 [30] P.J. Flory, *Principles of polymer chemistry*, Cornell University Press 1953.
- 494 [31] S. Havanur, V. Farheenand, P. JagadeeshBabu, Synthesis and optimization of poly (N, N-
495 diethylacrylamide) hydrogel and evaluation of its anticancer drug doxorubicin's release behavior, *Iranian*
496 *Polymer Journal*, 28 (2019) 99-112.
- 497 [32] M. Sadeghi, B. Heidari, Crosslinked graft copolymer of methacrylic acid and gelatin as a novel
498 hydrogel with pH-responsiveness properties, *Materials*, 4 (2011) 543-552.
- 499 [33] F.L. Buchholz, N.A. Peppas, *Superabsorbent polymers: science and technology*, ACS
500 Publications 1994.
- 501 [34] H. Omidian, S. Hashemi, P. Sammes, I. Meldrum, A model for the swelling of superabsorbent
502 polymers, *Polymer*, 39 (1998) 6697-6704.
- 503 [35] R. Ebrahimi, The study of factors affecting the swelling of ultrasound-prepared hydrogel, *Polymer*
504 *Bulletin*, 76 (2019) 1023-1039.

505

